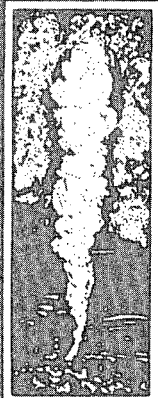


**PROCEEDINGS
NINTH WORKSHOP
GEOTHERMAL RESERVOIR ENGINEERING**

December 13-15, 1983



**Henry J. Ramey, Jr., Paul Kruger, Frank G. Miller,
Roland N. Horne, William E. Brigham,
and Jon S. Gudmundsson
Stanford Geothermal Program
Workshop Report SGP-TR-74***

DISCLAIMER

This report was prepared as an account of work sponsored by an agency of the United States Government. Neither the United States Government nor any agency Thereof, nor any of their employees, makes any warranty, express or implied, or assumes any legal liability or responsibility for the accuracy, completeness, or usefulness of any information, apparatus, product, or process disclosed, or represents that its use would not infringe privately owned rights. Reference herein to any specific commercial product, process, or service by trade name, trademark, manufacturer, or otherwise does not necessarily constitute or imply its endorsement, recommendation, or favoring by the United States Government or any agency thereof. The views and opinions of authors expressed herein do not necessarily state or reflect those of the United States Government or any agency thereof.

DISCLAIMER

Portions of this document may be illegible in electronic image products. Images are produced from the best available original document.

ANALYSIS OF PRODUCTION DATA
FROM THE KRAFLA GEOTHERMAL FIELD, ICELAND

K. Pruess and G.S. Bodvarsson
Earth Sciences Division
Lawrence Berkeley Laboratory
University of California
Berkeley, California 94720

V. Stefansson
National Energy Authority of Iceland
Reykjavik, Iceland

Introduction

The Krafla geothermal field in northeastern Iceland consists of several zones, which contain fluids of different composition and thermodynamic state (Stefansson, 1981). In this paper we examine production data from wells which are completed in two-phase zones. Transient changes in flow rate and flowing enthalpy are analyzed to obtain insight into relative (liquid and gas phase) permeabilities, and other reservoir parameters.

Numerous studies have shown that predictions of geothermal reservoir behavior are strongly dependent upon the choice of relative permeability functions. There is an extensive literature on gas-oil and oil-water relative permeabilities, but steam-water relative permeabilities which are needed for geothermal reservoir analysis are poorly known. Laboratory experiments by Chen et al. (1978) and Counsil and Ramey (1979) have provided some data which, however, seem to be at variance with relative permeability characteristics deduced from field data by Grant (1977) and Horne and Ramey (1978). The differences may reflect uncertainties in the analysis methods used, or they may reflect "real" differences in relative permeability behavior of fractured reservoirs from that of porous medium-type laboratory cores. Recent theoretical work by Menzies (1982) and Gudmundsson et al. (1983) has substantiated the relative permeability characteristics obtained by Horne and Ramey (1978) for Wairakei wells.

Production Data

Krafla wells completed in two-phase zones show strong transients in flow rate and enthalpy when first put on production. As a typical example of this behavior, Figure 1 shows production data from well 12. Initially the well produced approximately 14 kg/s of water and 20 kg/s of steam from a reservoir at a temperature of approximately 320°C. Within a few days water production ceased, and steam production dropped to approximately 10 kg/s. After three months steam production had declined to 6 kg/s, while enthalpy continued to increase slowly.

The observed transients of flow rate and enthalpy are influenced by many reservoir properties in the vicinity of the well. In general, the main parameters governing well behavior are: permeability, porosity, effective wellbore radius (skin),

in-place vapor saturation, and relative permeability characteristics of the medium. Many of these properties may be spatially variable, and a priori knowledge of the relevant parameters is limited.

In Figure 2 we have plotted flow rate on a logarithmic scale versus flowing enthalpy for several Krafla wells completed in two-phase zones. When plotted in this fashion, most data points fall on smooth curves, with some approximately linear sections (Stefansson et al., 1982). The sizeable scatter of the data present in some cases for wells 12 and 14 occurs because of variations in well head pressure. We have drawn smooth curves through the data points, which for wells 12, 13, and 15 are approximately parallel. This indicates similar relative permeability characteristics for these wells. Well 14, which is completed in a different reservoir zone (Bodvarsson et al., 1983a), is operated at a much higher well head pressure, and shows a different correlation between flow rate and enthalpy.

Relative Permeability Analysis

We have used the smoothed field data (see Figure 2) to study the relative permeability behavior of wells 12 through 15. Our method of analysis is similar to that of Grant (1977), and can be summarized with the following equations. The flow rate of a two-phase well is written

$$q = PI(p - p_{wb}) \left[\frac{k_{rl} \rho_l}{\mu_l} + \frac{k_{rv} \rho_v}{\mu_v} \right] \quad (1)$$

Here PI is the productivity index of the well, p is an average reservoir pressure in the vicinity of the well, and p_{wb} is the flowing down-hole pressure. Parameters specific to the liquid phase are: relative permeability k_{rl} , density ρ_l , and viscosity μ_l , with analogous definitions applying to the vapor phase. The parameter group $PI(p - p_{wb})$ is identical to the parameter B used by Grant (1977).

Expressing flowing enthalpy as:

$$h = \frac{\frac{k_{rl}}{k_{rv}} \frac{\rho_l}{\mu_l} h_l + \frac{\rho_v}{\mu_v} h_v}{\frac{k_{rl}}{k_{rv}} \frac{\rho_l}{\mu_l} + \frac{\rho_v}{\mu_v}} \quad (2)$$

we have two equations relating the measured quantities q and h to the three unknowns k_{rl} , k_{rv} , and B . Grant (1977) obtained the needed third equation by considering a well which at some time was flowing at single-phase liquid conditions, in which case

$$q_l = B \frac{\rho_l}{\mu_l} \quad (3)$$

To obtain B -values for other wells, Grant shifted their log q vs. h -plots to obtain the best common plot. In our case this step is not necessary, because all wells considered here did actually reach single-phase (vapor) flow conditions, so that the vapor form of equation (3) can be used directly. The relative permeabilities obtained on this basis, assuming an average reservoir temperature of $T = 300^\circ\text{C}$, are plotted versus flowing enthalpy in Figure 3. The curves for different wells are rather different, with well 12 relative permeabilities generally considerably larger than those for the other wells.

The above analysis was based on the assumption that B is a constant parameter for each well, independent of flowing enthalpy. We suggest that this is a rather poor approximation, because both flowing downhole pressure p_{wb} and average reservoir pressure p near the well may vary considerably with flowing enthalpy. Using the smoothed data as shown in Figure 2, we compute B both for single-phase liquid ($h_l = 1344 \text{ kJ/kg}$) and for single-phase vapor ($h_v = 2749 \text{ kJ/kg}$). The results are given in Table 1. We then re-analyze the smoothed q vs. h data, using equations (1) and (2) with linear interpolation for the well indices between their liquid and vapor values:

$$\begin{aligned} B(h) &= [\rho_l (p - p_{wb})]_h \\ &= B_l + \frac{h - h_l}{h_v - h_l} [B_v - B_l] \end{aligned} \quad (4)$$

Figure 4 shows that with this renormalization the relative permeabilities for wells 12, 13, and 15 practically collapse into single curves. This provides evidence that the relative permeabilities for these wells are in fact virtually identical, and that the approximation made in (4) is valid. Well 14 shows a somewhat different behavior, which may indicate a true difference in relative permeability characteristics between different reservoir zones.

Inspection of Figure 4 shows that $k_{rl} + k_{rv} \approx 1$ to a good approximation over the entire range $h_l < h < h_v$. A similar conclusion was reached by Bodvarsson et al. (1983b), based on observed transients in steam rate at the separators for well 13, in response to injection into nearby well 7. It is also interesting to note that the shape of the relative permeability curves is rather similar to the theoretical streamtube model predictions of Menzies (1982) and Gudmundsson et al. (1983).

It should be emphasized that the relative permeability information obtained from the above analysis remains incomplete. Figure 4 displays relative permeabilities as functions of flowing enthalpy. However, for applications in geothermal reservoir modeling it is necessary to express relative permeability as a function of thermodynamic state variables, such as in-place vapor saturation. The relationship between S and flowing enthalpy h is unknown, so that the relative permeabilities as given in Figure 4 cannot be used in a numerical model. In fact, any relative permeability functions $k_{rl}(S)$, $k_{rv}(S)$ with $k_{rl} + k_{rv} = 1$ and monotonic dependence upon S are consistent with the results of our analysis.

Modeling of flow rate and enthalpy transients

The foregoing relative permeability analysis employed only the observed correlation between flow rates and enthalpies. The actual temporal variation of q and h did not enter into the discussion. Here we shall examine the transients as observed for well 12 (see Figure 1) to deduce further information about reservoir parameters and conditions.

We have used our numerical simulators SHAFT79 (Pruess and Schroeder, 1980) and MULKOM (Pruess, 1983) to model the time dependence of flow rate and enthalpy. As a first approach we use the field-measured flow rates as input to the simulator, and attempt to match the observed enthalpy transients. Table 2 shows parameters which were kept fixed in the simulations. Assuming uniform initial vapor saturation, we made an extensive parameter search for porosity, permeability, effective formation thickness, and relative permeability, using both porous and fractured porous medium models. This particular effort failed to produce anything resembling the observed enthalpy transient. The main shortcoming of all models with uniform vapor saturation is that they predict a much more rapid rise in enthalpy than is observed in the actual test. This discrepancy suggests that vapor saturation at the time when well 12 was opened for discharge was in fact nonuniform, with smaller values near the well.

A possible explanation for a nonuniform saturation distribution may be found in the drilling and completion practice. During drilling the reservoir region around the bore is cooled by circulating drilling fluid, which may cause some steam condensation in the formation. Furthermore, at the end of the drilling process cold water is continuously injected for a few days during well logging, testing, and stimulation. The average total mass of injected water has been estimated as 3000-5000 tonnes (Benediktsson, personal communication, 1982). Subsequently the well heats up for several weeks before being placed on production. If steam condensate and injected water remain in the vicinity of the bore rather than being dispersed over a larger reservoir region, this would provide an explanation for a non-uniform initial vapor saturation. Changes in the N_2/H_2 ratio of produced waters show that indeed for several days after placing a well on production a mixture of injected and reservoir waters is produced (Gislason et al., 1978).

Based on these considerations a conceptual model was developed in which the bulk of the reservoir has a "background" vapor saturation S_b , while near the well the initial vapor saturation is $S_n < S_b$. The "excess mass" present near the well due to steam condensation and cold water injection is

$$M_{ex} = V_n \phi (S_b - S_n)(\rho_\ell - \rho_v) \quad (5)$$

where V_n is the volume of the zone with $S=S_n$. Because of this excess mass enthalpy transients would be slower, as indicated by the field data. The radius of the "near-zone" V_n , which contains the excess mass and is in high-permeability contact with the well, was rather arbitrarily fixed at $R_n = 10$ m (corresponding to a negative skin value of $s = -4.5$). By varying relative permeability functions and porosity in the near-zone, several excellent matches to the enthalpy transients were obtained. Examples are shown in Figure 5, while Table 3 gives the key parameters for different cases.

It is apparent that the data can be matched equally well with different values for irreducible water saturation and initial vapor saturation. The different cases all agree closely in the excess mass present near the well, which also agrees well with the total amount of water injected. This together with the good quality of the enthalpy match gives strong support for the conceptual model employed in the simulations.

Despite the success of the model in matching field data it provides only rather limited insight into reservoir parameters. It does show clearly that the injected water remains near the well for a period of weeks. Furthermore, the water is in high-permeability contact with the wellbore. However, none of the important reservoir parameters, such as porosity, volume of the near-zone, initial vapor saturation in the near zone, functional form of relative permeabilities, and irreducible saturations, are uniquely defined.

Deliverability Model

The model discussed in the previous section employs part of the test data (time-dependent flow rates) to predict the enthalpy transients. While this has yielded a good match and a consistent description, it is desirable to develop a more comprehensive model in which all test data are matched with calculated values rather than prescribing some as input.

Here we present results from a "deliverability model", in which production rate depends upon reservoir pressure according to equation (1). Thus the time-dependence of both flow rate and enthalpy is predicted by the simulator. Evaluating equation (1) for single-phase vapor flow, using $q_v = 10$ kg/s, $p_{wb} = 2.0$ MPa, $p = 10.7$ MPa, we obtain $PI = 3.8 \times 10^{-13} \text{ m}^3$. The permeability-thickness product was fixed at the value 1.20 dm obtained from injection tests (Bodvarsson et al., 1983a). Using different relative permeability functions, and different values for vapor saturation, reservoir porosity, and radius R_n of the near zone with excess liquid

(see Table 4), we have been able to obtain a number of excellent matches to both flow rate and enthalpy (see Figures 6 and 7).

It turns out that the match is very sensitive to the choice of porosity and of S_n . Different choices of R_n can be compensated for by making appropriate adjustments in ϕ , such that ϕR_n^2 remains constant. The value of S_b must correspond to immobile or nearly immobile liquid, and is determined to within 5-10%. The excess mass present near the well due to condensation and injection is estimated as approximately 4.5×10^6 kg in most cases, which agrees very well with the injected mass. For Corey relative permeability functions a significantly larger M_{ex} is obtained than for linear functions. The quality of the fit for $[q(t), h(t)]$ is good in all cases, indicating that the transients are very sensitive to the excess mass, but not sensitive to the functional form of $k_{rl}(S)$ and $k_{rv}(S)$.

Conclusions

Our analysis of flow rate and enthalpy data from several wells completed in the same two-phase zone of Krafla geothermal reservoir has yielded consistent relative permeability parameters. We find that $k_{rl} + k_{rv} = 1$ over the entire range of two-phase flow conditions from immobile liquid to immobile vapor. The available data provide relative permeability parameters as a function of flowing enthalpy only. The relationship between flowing enthalpy and in-place vapor saturation remains unknown, so that the relative permeability information obtained is of limited value for quantitative modeling of geothermal reservoir performance.

Numerical simulation of flow rate and enthalpy transients has yielded excellent matches to production data from well 12. However, there is little information about the reservoir which can be deduced in an unambiguous way, because the field data could be matched with a variety of rather different parameter choices. The only unambiguous piece of information obtained is that the water injected into the well during drilling and completion remains in the vicinity of the wellbore during several weeks of warmup.

Acknowledgement

This work was supported by the State Electric Power Works of Iceland, and by the Assistant Secretary for Conservation and Renewable Energy, Division of Geothermal Energy and Hydropower Technologies of the U.S. Department of Energy under Contract No. DE-AC03-76SF00098.

References

Bodvarsson, G.S., Benson, S.M., Sigurdsson, O., Stefansson, V., and Eliasson, E.I., "The Krafla Geothermal Field, Iceland. 1. Analysis of Well Test Data", submitted to Water Resources Research, 1983a.
 Bodvarsson, G.S., Pruess, K., and O'Sullivan, M. J. "Injection and Energy Recovery in Fractured Geothermal Reservoirs", paper SPE-11689, presented at the California Regional Meeting of the SPE, Ventura, Ca., March 1983b.

Chen, H.K., Counsil, J.R., and Ramey, H.J., Jr.
 "Experimental Steam-Water Relative Permeability Curves", GRC Transactions, Vol. 2, p. 103, July 1978.

Counsil, J.R., and Ramey, H.J., Jr.
 "Drainage Relative Permeabilities Obtained from Steam-Water Boiling Flow and External Gas Drive Experiments, GRC Transactions, Vol. 3, p. 141-143, September 1979.

Gislason, G., Armannsson, H., and Hauksson, T. "Krafla-Hitaastand og Gastegundir i Jardhittakerfinu, National Energy Authority, OSJHD-7846, 1978.

Grant, M.A. "Permeability Reduction Factors at Wairakei", paper 77-HT-52, presented at AICHE - ASME Heat Transfer Conference, Salt Lake City, Utah, August 1977.

Gudmundsson, J.S., Menzies, A.J., and Horne, R.N. "Streamtube Relative Permeability Functions for Flashing Steam-Water Flow in Fractures", paper SPE-11686, presented at the 1983 California Regional Meeting, Ventura, Ca., March 1983.

Horne, R.N., and Ramey, H.J., Jr.
 "Steam-Water Relative Permeabilities from Production Data", GRC Transactions, Vol. 2, p. 291-293, July 1978.

Menzies, A.J., "Flow Characteristics and Relative Permeability Functions For Two-Phase Geothermal Reservoirs From A One Dimensional Thermodynamic Model", Stanford Geothermal Program, Report SGP-TR-59, 1982.

Pruess, K., "Development of the General Purpose Simulator MULKOM", Annual Report 1982, Earth Sciences Division, Lawrence Berkeley Laboratory, 1983.

Pruess, K., and Schroeder, R.C.
 "SHAFT79 User's Manual", Lawrence Berkeley Laboratory Report LBL-10861, Berkeley, Ca.,

Stefansson, V., "The Krafla Geothermal Field, Northeast Iceland", in: Geothermal Systems, L. Rybach and L.J.P. Muffler (eds.), p. 273-294, 1981.

Stefansson, V., Gudmundsson, A., Steingrimsson, B., Armannsson, H., Franzson, H., Sigurdsson, O., and Hauksson, T., "Krafla Well KJ-13", Report by the Icelandic Energy Authority, OS82046/JHDU7, 1982.

Table 1. Well indices.

| Well | Well Index B (10^{-6} Pa \cdot m 3) | |
|------|---|-------|
| | Liquid | Vapor |
| 12 | 8.3 | 4.1 |
| 13 | 3.1 | 2.5 |
| 14 | 4.4 | 5.7 |
| 15 | 1.7 | 1.6 |

Table 2. KG-12 Simulations - Fixed Parameters

| Parameter | Value |
|------------------------------|---|
| produced flowrate | as observed in the field (time-dependent) |
| reservoir temperature | 320°C |
| reservoir pressure | 112.89 bars (=saturation pressure at T=320°C) |
| rock density | 2650 kg/m 3 |
| rock specific heat | 1000 J/kg°C |
| rock heat conductivity | 2.0 W/m°C |
| skin | -4.5 |
| irreducible vapor saturation | 0 |

Table 3. Simulations with prescribed (observed) flow rate.

| parameter | Case 1 | Case 2 | Case 3 |
|--------------------------------|--------|--------|-----------------|
| kH (Dm) | 2.0 | 1.2 | 1.2 |
| relative permeability function | linear | Corey | smoothed linear |
| S_{lr}^* | .30 | .30 | .40 |
| S_{sr}^+ | .00 | .00 | .05 |
| $S_{pv}^{\#}$ | 1.00 | 1.00 | 0.65 |
| S_b | .70 | .50 | .65 |
| S_n | .45 | .30 | .38 |
| ϕ | .08 | .11 | .08 |
| $M_{ex}(10^6 \text{ kg})$ | 3.78 | 4.16 | 4.09 |

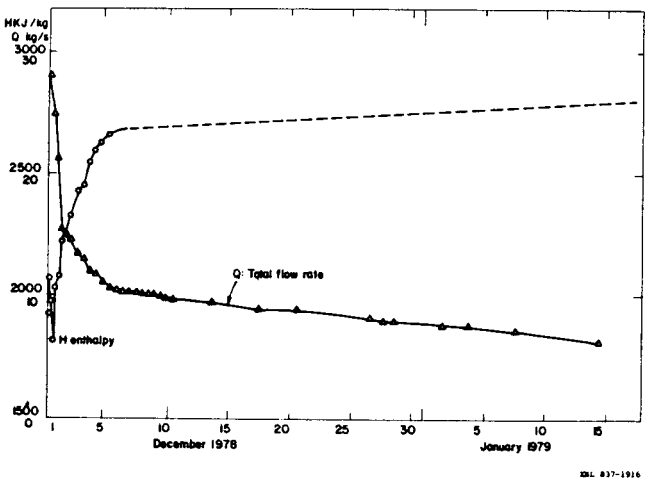
*irreducible liquid saturation

+irreducible vapor saturation

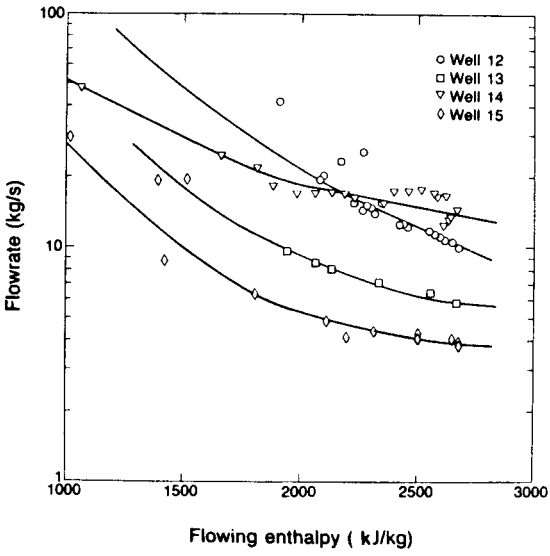
#perfectly mobile vapor saturation

Table 4. Simulations using a deliverability model.

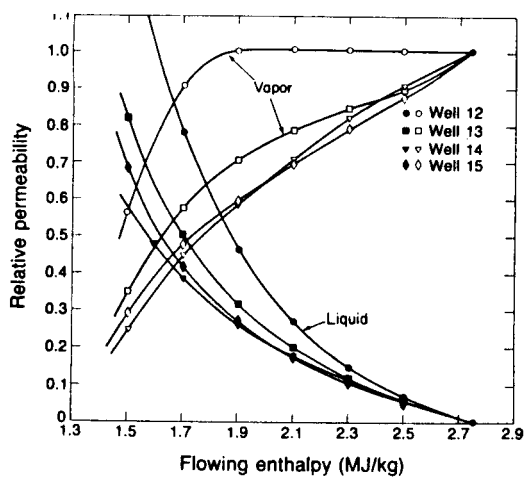
| Parameter | Case 1 | Case 2 | Case 3 | Case 4 |
|--------------------------------|-----------------|-----------------|--------|-----------------|
| relative permeability function | smoothed linear | smoothed linear | Corey | smoothed linear |
| S_{lr} | .40 | .50 | .30 | .40 |
| S_{sr} | .05 | .05 | .0 | .05 |
| S_b | .65 | .55 | .50 | .65 |
| S_n | .24 | .16 | .06 | .24 |
| ϕ | .015 | .06 | .06 | .06 |
| R_n (m) | 20 | 10 | 10 | 10 |
| M_{ex} (10^6 kg) | 4.66 | 4.43 | 5.00 | 4.66 |



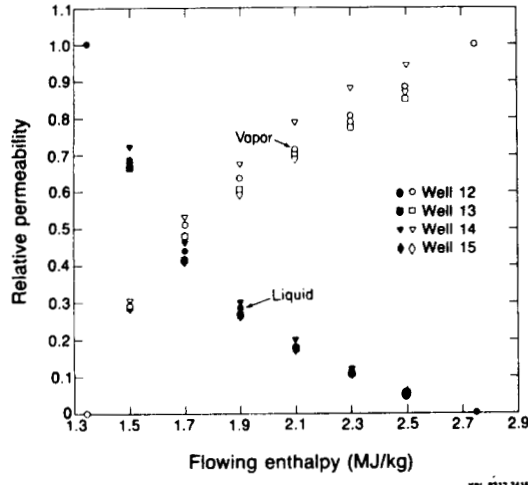
1. Production data for well 12.



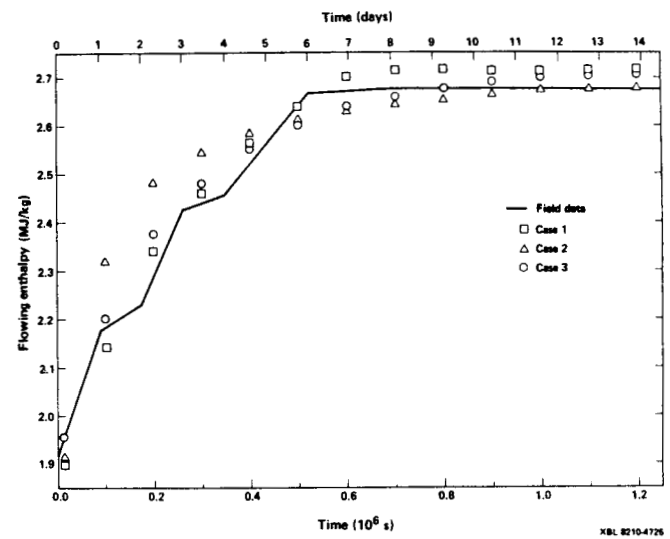
2. Observed correlation between flow rate and flowing enthalpy.



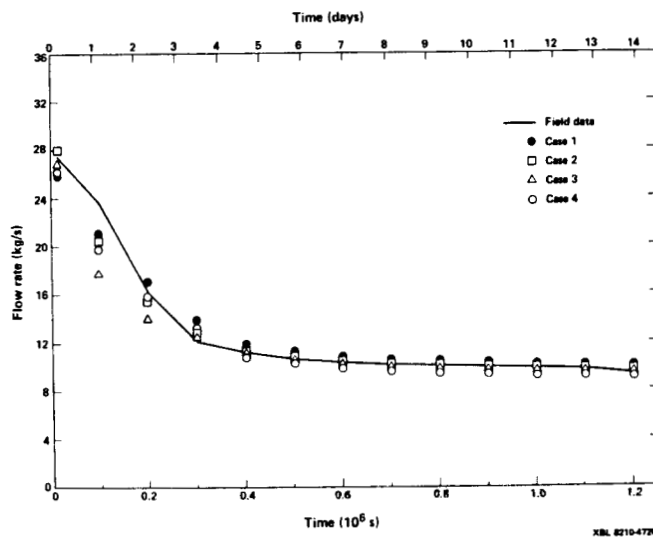
3. Relative permeabilities assuming constant well indices.



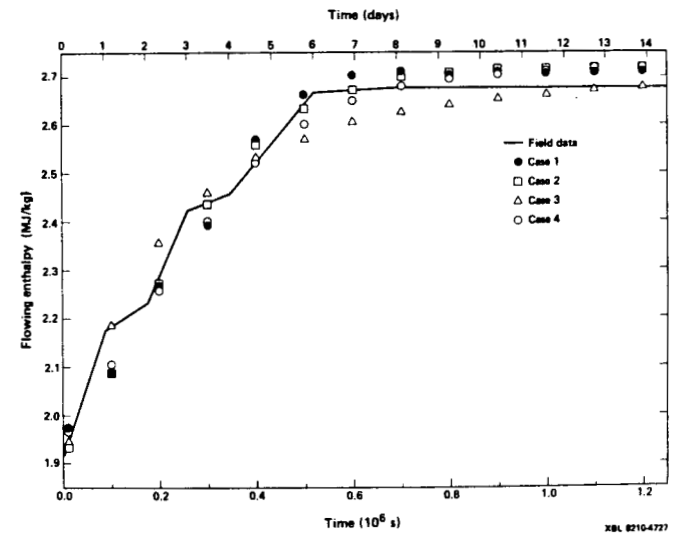
4. Renormalized relative permeabilities.



5. Comparison between calculated and observed enthalpies for well 12 (calculation uses observed flow rates).



6. Comparison between calculated and observed flow rates for well 12 (deliverability model).



7. Comparison between calculated and observed enthalpies for well 12 (deliverability model).